Dynamic Configuration of Coactive Micropatterns in the Default Mode Network during Wakefulness and Sleep

Yan Cui[1], Min Li[1], Bharat Biswal[1, 2, *], Wei Jing[1, 3], Changsong Zhou[4], Huixiao Liu[1], Daqing Guo[1, 6, *], Yang Xia[1], Dezhong Yao[1, 5, 6, *]

[1]The Clinical Hospital of Chengdu Brain Science Institute, MOE Key Lab for NeuroInformation, University of Electronic Science and Technology of China, Chengdu 611731, China

[2]Department of Biomedical Engineering, New Jersey Institute of Technology, Newark, NJ 07102, USA

[3]Department of Physiology, School of Basic Medicine and Tongji Medical College, Huazhong University of Science and Technology, Wuhan, China

[4]Department of Physics, Centre for Nonlinear Studies and Beijing-Hong Kong-Singapore Joint Centre for Nonlinear and Complex Systems (Hong Kong), Institute of Computational and Theoretical Studies, Hong Kong Baptist University, Kowloon Tong, Hong Kong

[5]School of Electrical Engineering, Zhengzhou University, Zhengzhou 450001, China

[6]Sichuan Institute for Brain Science and Brain-Inspired Intelligence, Chengdu 611731, China

[*]Corresponding authors: dqguo@uestc.edu.cn, dyao@uestc.edu.cn and bbiswal@gmail.com

Keywords: default mode network; coactive micropattern; wakefulness and sleep; up-down states; dynamic configuration

Abstract

The activity in the default mode network (DMN) rapidly fluctuates in different conscious states during wakefulness and sleep, indicating the high complexity of the DMN in consciousness. Tracking the dynamics of these fluctuations is critical for deeply understanding the physiological mechanism of consciousness. Herein, we address this issue by elucidating the dynamics of local field potentials (LFPs) of the rat DMN in different conscious stages during wakefulness and sleep. We novelly propose a coactive micropattern (CAMP) algorithm to evaluate the configurations of rat DMN dynamics, and further reveal the relationship between DMN dynamics with consciousness. From DMN gamma activity (40-80 Hz) across wakefulness and sleep, three spatially stable CAMPs were detected, a common low-activity level micropattern (cDMN), an anterior high-activity level micropattern (aDMN) and a posterior high-activity level micropattern (pDMN). A dynamic balance across CAMPs emerged during wakefulness and was disrupted in sleep stages. In the slow wave sleep (SWS) stage, the cDMN became the primary activity pattern, while the aDMN and pDMN were the major activity patterns of DMN activity in the rapid eye movement sleep (REM) stage. Additionally, further investigation revealed a certain level of phasic relationships between CAMPs and the up-down states of the slow DMN activity in the SWS stage. Our study reveals that the dynamic configurations of CAMPs were highly associated with consciousness levels, and provides a potential three-state model in DMN dynamics for consciousness during wakefulness and sleep.

Impact Statement

In the current study, a novel coactive micropattern method (CAMP) was developed to elucidate fast DMN dynamics during wakefulness and sleep. Our findings show that the dynamic configurations of DMN activity are specific to different conscious stages and provide a three-state DMN CAMP model to depict consciousness levels, thus revealing a potentially new neurophysiological representation of consciousness levels. This work could deepen our knowledge of the DMN dynamics underlying different conscious stages and have important implications for the theoretical understanding of the neural mechanism of consciousness during wakefulness and sleep.

Introduction

Multimodal imaging studies of the human brain have discovered that several intrinsic connectivity networks (ICNs) coexist during the resting state(Beckmann, DeLuca, Devlin, & Smith, 2005; Q. Liu, Farahibozorg, Porcaro, Wenderoth, & Mantini, 2017). Dynamic switching within these ICNs displays a hierarchical structure over time for brain activity at rest and is significantly associated with cognitive traits(M. D. Fox et al., 2016; Vidaurre, Smith, & Woolrich, 2017), suggesting that brain activity is appropriately understood in terms of the dynamic configuration among ICNs. These studies mainly consider each ICN as a whole during brain dynamics but ignore the intrinsic dynamics of individual ICNs. Indeed, individual ICNs also show strong fluctuations in brain activity, and different ICNs are believed to dominate distinct cognitive functions(Rosazza & Minati, 2011). For a specific brain function, further tracking the dynamic configuration of fluctuations in brain activity at the single-ICN level might be critical for revealing the underlying physiological mechanism.

As a task-negative ICN, the default mode network (DMN) has been consistently reported to be less active during attention-demanding tasks, while high activation of DMN could be observed at rest(Gusnard, Akbudak, Shulman, & Raichle, 2001; M E Raichle et al., 2001). Further investigations highlighted and refined the DMN as the key neural correlate of consciousness in humans and rodents(K. C. R. Fox, Foster, Kucyi, Daitch, & Parvizi, 2018; Lu et al., 2012; Marcus E Raichle, 2015). DMN connectivity between the frontal and posterior areas in the human brain is reduced

during the slow wave sleep (SWS) stage(Sämann et al., 2011), during which a low level of consciousness is displayed. However, at sleep onset and throughout the rapid eye movement sleep (REM) stage of primary consciousness(Hobson, 2009), the regions in the human DMN were shown to be persistently coupled(Horovitz et al., 2008; Larson-Prior et al., 2009). These findings illustrate that DMN activity is functionally reorganized during sleep and might further reflect levels of consciousness. Additionally, fast and ever-changing dynamics of DMN activity have also been observed in various consciousness levels in humans, and the temporal aspects of spontaneous DMN activity might be associated with conscious processes(Kapogiannis, Reiter, Willette, & Mattson, 2014; Panda et al., 2016). Therefore, the close association between DMN activity and consciousness represents an important topic for better understanding the physiological mechanism of consciousness by revealing the dynamic configuration of fast DMN activity, which has not been completely elucidated.

The DMN is also observable in rat brains, indicating its conservation in the mammalian brain during evolution(Huang et al., 2016; Lu et al., 2012). Though the anatomical topology of rat DMN is visually similar to that of the human DMN, and both can be fractionated into anterior and posterior subsystems; some differences do exist(Hsu et al., 2016; Marcus E Raichle, 2015). The lateral parietal component of the human DMN lies approximately in the Brodmann area 39, while that in the rat DMN resides in the parietal association cortices, which include the posterior parietal cortex and the secondary visual cortex. In addition, activated DMN regions were also

observed in awake rats, and suppressing the activity in the core DMN region could modulate a rat's normal behavior(Tu, Ma, Ma, Dopfel, & Zhang, 2020; Upadhyay et al., 2011). Furthermore, the information flow within anterior and posterior DMN subsystems showed various alterations in different sleep states and mental disorders in rats(Cui et al., 2018; Jing et al., 2017). All these findings imply that the rat DMN also supports a variety of self-referential functions, and employing rat models to investigate the neurobiological basis of the DMN thus makes sense.

During the deep sleep state, recent neurophysiological studies discovered that the neurons in various brain regions exhibited highly synchronized firing rates, occurring at approximately 0.5-2 Hz(Crunelli & Hughes, 2010; Gretenkord et al., 2020; Lőrincz et al., 2015). This specific activity pattern was identified as the up-down state, which has progressively been considered a biomarker of low-level consciousness(Jercog et al., 2017; Perez-Zabalza et al., 2020). Moreover, this up-down state has been shown in regards to both neuron membrane potentials and local field potentials (LFPs)(Holcman & Tsodyks, 2006) and characterizes the dynamics of slow oscillations during deep sleep(Ji & Wilson, 2007; Lőrincz et al., 2015). However, researchers are still debating the existence of a physiological relationship between the up-down state and DMN dynamics, constituting another issue that deserves further exploration.

In the present study, we developed and applied a new dynamic activity pattern method to address these challenges. The proposed method elucidated the dynamic configurations of fast neural activity in different conscious stages based on the

coactive patterns in envelope activity from multichannel physiological signals. The new method, coactive micropattern analysis (CAMP), decomposed the dynamics of neural activity into several intrinsic CAMPs and defined the configurations across time through the constitutions and transitions among these CAMPs. We then applied CAMP analysis to the recorded LFPs from rat DMN during wakefulness and sleep. Our results demonstrated the reorganized dynamic configurations of CAMPs for fast DMN activity in different conscious stages, implying that the dynamic configurations of DMN micropatterns might provide underlying neural correlates for the consciousness levels observed during wakefulness and sleep.

Methods and Materials

Detailed descriptions of the experimental procedures and data acquisition are described in the ***Supplementary Materials.*** Twenty-nine male Sprague-Dawley rats were used in our experiment. The DMN signals were acquired by chronically implanting fifteen electrodes into the brains of rats under deep anesthesia (Fig. 1 and Table 1). The rat DMN contained the following bilateral structures: the orbital frontal cortex (OFC), the rostral dorsal prelimbic cortex (PrL), the cingulate cortex (CG), the retrosplenial cortex (RSC), the dorsal hippocampus (HIP), the temporal lobe (TE), the medial secondary visual cortex (V2) and the posterior parietal cortex (PPC). According to their anatomical coordinates(Lu et al., 2012), the PrL, OFC and CG regions were considered to be in the anterior subsystem of the DMN, while the RSC, HIP, PPC, TE and V2 regions were in the posterior subsystem of the DMN. During

the recording session, the rats were placed in a noise-attenuated chamber, and the LFP signals were continuously monitored for 72 h. The dataset used in the current study was selected from the last 24 h of the total recording and was separated into three stages, including resting (AWAKE), SWS and REM sleep stages. For each rat, 30 segments in different stages were chosen, and each segment lasted 10 s (a total of 300 s of LFPs). All experimental animal procedures were approved by the Institutional Animal Care and Use Committee of the University of Electronic Science and Technology of China.

Moreover, we proposed a novel CAMP method to track fast DMN dynamics during wakefulness and sleep. Briefly, this method utilizes a point process approach that combines the advantages of both microstate analysis and coactive pattern analysis(X. Liu & Duyn, 2013; Michel & Koenig, 2018) and extracts CAMPs based on the extreme values of envelope signals at a high temporal resolution. Five steps were included in the CAMP algorithm. First, the original data were bandpass filtered into the gamma frequency band (40-80 Hz) and then subjected to Hilbert transformation to obtain the envelope signals (Fig. 2b). Second, the envelope signals were normalized and downsampled to improve the signal-to-noise ratio (SNR) for further analysis (Fig. 2c). Third, the active points for each envelope signal channel were then defined as the extreme points of the envelope signals, including local maximum and minimum values. Afterwards, the coactive patterns (CAPs) of the brain, defined as the brain maps in which more than one brain region displayed active points at the same time point, were introduced for all stages (Fig. 2d). Fourth, the k-means

clustering algorithm was applied to all the CAPs to decompose the CAMPs and the CAMP index (Fig. 2e). Last, the criterion based on squared Euclidean distance was applied to update the CAMP and CAMP index (Fig. 2f). The last step was employed to precisely determine the final spatial structures of all CAMPs and the CAMP index. With the CAMP method, we decomposed three stable CAMPs from gamma activity during DNMN dynamics to reveal the fast changes in DMN activity in different conscious stages. A detailed description of the CAMP analysis is provided in the ***Supplementary Methods***.

The CAMP method was separately applied to the DMN activity of each segment in different conscious states for each rat, and to the concatenated DMN activity of all rats and all stages during wakefulness and sleep. The CAMPs extracted from each rat in different conscious stages were further employed to test their spatial stability across rats and consciousness levels with Pearson correlation coefficient method. The results were derived from the CAMPs extracted from the concatenated DMN activities from all rats during wakefulness and sleep unless otherwise described.

Results

Three CAMPs of gamma activity in the DMN during wakefulness and sleep. The CAMP analysis procedure developed in the present study is schematically illustrated in Fig. 2 and in the ***Supplementary Methods***. The concatenated gamma activities in the DMNs of all rats and all stages during wakefulness and sleep were decomposed into three distinct CAMPs, including a common low-activity level micropattern

(cDMN), an anterior high-activity level micropattern (aDMN) and a posterior high-activity level micropattern (pDMN). In the cDMN, all DMN regions showed similar and low levels of activity (mean normalized activity: 0.2577 ± 0.0041, Fig. 2g), indicating a potential cooperation of these regions in this type of CAMP. However, two different levels of activity were observed in both the aDMN and pDMN, with the aDMN exhibiting relatively higher levels of activity in the anterior DMN regions (mean normalized activity: 0.3868 ± 0.0018) and lower activity in the posterior DMN structures (mean normalized activity: 0.3050 ± 0.0060, Fig. 2h). In the pDMN, the posterior DMN structures displayed higher levels of activity (mean normalized activity: 0.3793 ± 0.0145), while the anterior DMN regions showed relatively lower levels of activity (mean normalized activity: 0.3073 ± 0.0021, Fig. 2i). Accordingly, both the aDMN and pDMN were considered high-activity micropatterns in DMN dynamics.

We separately decomposed the CAMPs for each rat in every conscious stage individually, and tested their reliability across rats and conscious stages. All three CAMPs exhibited high stability with large correlation coefficients among different rats during wakefulness and sleep (mean correlation coefficients: r = 0.7451, r = 0.7535, r = 0.6684 for the AWAKE, SWS and REM sleep stages, respectively; Table 2). In addition, the spatial structures of these CAMPs were also similar among the AWAKE, SWS and REM sleep stages (mean correlation coefficients: r = 0.6229, r = 0.7882, r = 0.8600 for the AWAKE, SWS and REM sleep stages, respectively; Table 3). These findings demonstrated the high reliability and robustness of these CAMPs.

Temporal features and activity levels of each CAMP during wakefulness and sleep. We computed several temporal measurements, including the total occurrence (occurrence probability), total duration (duration probability) and mean duration, to characterize the features and dynamics of these CAMPs during wakefulness and sleep. All these features represented the temporal properties of these CAMPs in different conscious stages. Based on the comparisons, all features of the low-activity micropattern cDMN displayed the largest values in the SWS stage and the smallest values in the REM sleep stage, and the two high-activity micropatterns (aDMN and pDMN) exhibited the largest values for all features in the REM sleep stage and the smallest values in the SWS stage (Fig. 3a-3c). These opposite alterations in features between low- and high-activity micropatterns were also highly significant, suggesting that these two types of CAMPs observed in DMN dynamics represent different physiological characteristics of consciousness during wakefulness and sleep. The CAMP features in different conscious stages were remarkable and help improve our knowledge of the changes in consciousness during wakefulness and sleep.

However, all of these CAMPs displayed different activities in DMN regions during wakefulness and sleep. In particular, all DMN regions exhibited reduced activity during SWS stages in all CAMPs (Fig. 3e-3g). Moreover, the posterior DMN structures exhibited significantly reduced activity in the aDMN, while the anterior DMN regions exhibited significantly reduced activity in the pDMN; all these regions showed relatively lower activity in the AWAKE stage. The significantly decreased activity in the regions with lower level activity in the two high-activity micropatterns

indicated a preservation of the major activity in these two micropatterns during deep sleep (Fig. 3f-3g, red stars). However, all CAMPs displayed increased activity in most DMN regions during the REM sleep stage. The activities in the HIP, OFC and RSC regions were significantly increased during the REM sleep stage in all CAMPs, implying the importance of these DMN regions for REM sleep (Fig. 3h-3j, red stars). In addition, the mean activity level of each CAMP exhibited similar variation trends across different conscious stages. The lowest mean activity of CAMPs was observed in the SWS stage, while the highest mean activity was observed in the REM sleep stage (Fig. 3d).

The constitutions and transitions of CAMPs during wakefulness and sleep. The configurations of these CAMPs involved in DMN dynamics in different conscious stages were also distinct (Fig. 4a-4c). All CAMPs presented similar features in the AWAKE stage (occurrence probabilities: 32.12%, 34.12% and 33.75%; duration probabilities: 31.68%, 34.15% and 34.17%; and mean duration: 29.79 ms, 24.41 ms and 24.37 ms for the cDMN, aDMN and pDMN, respectively. No significant differences in any features were observed, indicating that their roles were equivalent and that a dynamic balance in DMN activity might exist among CAMPs at wakeful rest. However, the cDMN became the dominant activity pattern of DMN dynamics in the SWS stage, as it had the largest occurrence probabilities (62.66%, 17.56% and 19.78% for the cDMN, aDMN and pDMN, respectively), duration probabilities (61.47%, 18.02% and 20.51% for the cDMN, aDMN and pDMN, respectively) and mean duration (55.58 ms, 21.89 ms and 22.78 ms for the cDMN, aDMN and pDMN,

respectively) among all CAMPs. The predominant constituent of the low-activity micropattern suggested that all the DMN regions might have been in a state of low activity and that the DMN activity preferred a silent pattern during deep sleep. Unlike the SWS stage, the two high-activity micropatterns were the main CAMPs observed in the REM sleep stage, as indicated by the remarkably larger values for all features of the aDMN and pDMN than the cDMN (occurrence probabilities: 19.42%, 42.05% and 38.53%; duration probabilities: 19.33%, 41.84% and 38.83%; and mean duration: 21.88 ms, 26.92 ms and 26.01 ms for the cDMN, aDMN and pDMN, respectively). The greater percentage of high-activity micropatterns during REM sleep suggested a reactivation of DMN activity in this consciousness stage. In addition, comparison of the two high-activity micropatterns demonstrated that the aDMN displayed significantly larger values for the three features, implying that it plays a more important role in REM sleep.

Furthermore, the temporal concatenations of these CAMPs (i.e., the CAMP indices) in different conscious stages also showed specific changes. We first performed a randomization test to examine the transition structures of these CAMP indices in different stages. The transitions among CAMPs occurred randomly in the AWAKE stage ($p = 0.8157$), indicating that the transition probabilities (TPs) of pairs of CAMPs in the resting state were proportional to their occurrences. However, these transitions did not occur randomly in the SWS ($p<0.0001$) or REM sleep stages ($p<0.0001$), which suggested the stabilization of the CAMP index structures during the sleep cycle and further implied the existence of several preferred transitions

among CAMPs in the SWS and REM sleep stages.

Next, we compared the TPs for pairs of CAMPs between the two sleep stages and the AWAKE stage and revealed similar TPs in the AWAKE stage (no significant differences among all TPs, Fig. 4d), suggesting the presence of balanced state transitions among all CAMPs at rest. However, the TPs within the two high-activity micropatterns showed significant reductions in the SWS stage, while those between high-activity micropatterns and the low-activity micropattern increased significantly (Fig. 4e). These changes in TPs emphasized the functional role of inhibitory activity in DMN regions in deep sleep. On the other hand, the TPs in the REM sleep stage displayed different alterations than those in the SWS stage, including significantly increased TPs within high-activity micropatterns and a remarkable decrease in TPs between high-activity micropatterns and the low-activity micropattern (Fig. 4f). The increased transitions within the two high-activity micropatterns revealed increased activation of DMN regions during REM sleep. Based on these findings, the CAMP indices and the functional roles of these CAMPs were specific for different conscious stages. The alterations in DMN activity during wakefulness and sleep might be attributed to the specific temporal combinations of the CAMPs constituting the activity in different conscious stages rather than the spatial structures of CAMPs themselves, which were rather stable across different stages.

Strong phasic relationships between CAMPs and the up-down states in the SWS stage. Up-down states are considered the predominant pattern of slow oscillations (0.5-2 Hz) during the SWS stage. Estimations of the phase distributions of each

CAMP in the anterior and posterior DMN slow activity regions with the Hilbert transformation demonstrated that these CAMPs displayed strong phasic relationships with the up-down states in the SWS stage. The cDMN preferred the down state of anterior DMN activity (Fig. 5a, significant directionality: 1.97π, red line) and the up state of posterior DMN activity (Fig. 5d, significant directionality: 1.16π, red line). Additionally, both the aDMN and pDMN were phase locked to the up state of anterior DMN activity (Fig. 5b, significant directionality: 1.21π for aDMN; Fig. 5c, significant directionality: 1.18π for pDMN) and the down state of posterior DMN activity (Fig. 5e, significant directionality: 0.23π for aDMN; Fig. 5f, significant directionality: 0.18 π for these two high-activity micropatterns that might belong to the same activity pattern of slow pDMN), implying oscillations of the DMN during deep sleep. Furthermore, the difference in the significant directionalities of all CAMPs suggested that the slow oscillations in the anterior and posterior DMN regions tended to have a phasic shift of approximately π during deep sleep. Accordingly, our proposed CAMPs could also reflect the up-down states of DMN slow activity in the SWS stage, and a close physiological association existed between the up-down states of DMN dynamics.

Discussion

In the present study, we proposed and applied a coactive micropattern algorithm to reveal the dynamics of gamma activity in the rat DMN during wakefulness and sleep. Our results indicated that the fast dynamics of gamma activity in the DMN were decomposed into three different CAMPs in different conscious stages. These

CAMPs showed stable spatial structures across wakefulness and sleep, while their dynamic configurations were specific to different conscious stages. In addition, all these CAMPs were strongly phase locked to the up-down states in the SWS stage, suggesting the temporal sequence of the neural relationship between up-down states and DMN dynamics. Our findings described the distinct dynamic configurations of gamma activity in the DMN during wakefulness and sleep and proposed a three-state model to reveal the fundamental neural mechanism by which DMN dynamics mediate consciousness.

Physiological significance of the three CAMPs. Previous studies have reported a strong correlation between electrophysiological gamma activity and blood oxygen level-dependent (BOLD) signals(N. K. Logothetis, Pauls, Augath, Trinath, & Oeltermann, 2001; Nikos K. Logothetis, 2002; Magri, Schridde, Murayama, Panzeri, & Logothetis, 2012; Scheering, Koopmans, Van Mourik, Jensen, & Norris, 2016). In addition, DMN regions have also shown deactivation at gamma frequency during the performance of external tasks in several human electroencephalography (EEG) studies(Karim Jerbi*† et al., 2010; Ossandon et al., 2011), indicating the importance of gamma oscillation in DMN activity. Hence, we specifically focused on the fast dynamics of gamma activity in the DMN in the current study. Besides, we also showed the CAMPs decomposed from DMN alpha (8-13Hz) and beta (13-30Hz) activity, which are important frequency bands during wakefulness-sleep cycle. We found that there were also three CAMPs in the DMN dynamics of alpha and beta bands, and these CAMPs exhibited similar spatial structures with those found in

gamma band (Supplementary Fig. 5). The gamma activity in the rat DMN was decomposed into three stable CAMPs during wakefulness and sleep that exhibited distinct spatial structures. The differences in these CAMPs provided direct electrophysiological evidence that the DMN regions might not be activated simultaneously. Moreover, all these CAMPs lasted for approximately forty milliseconds and had distinct periods. These phenomena exhibited differences in the activation times of anterior and posterior DMN structures in the fast dynamics and further illustrated the diversity in the latencies for both the excitation and inhibition of DMN regions(Brett L. Foster, Mohammad Dastjerdi, 2012; Foster, Rangarajan, Shirer, & Parvizi, 2015).

Indeed, both human and animal studies found that the structure of DMN could be separated into two subnetworks, including a parietal subnetwork and a prefrontal subnetwork(Cui et al., 2018; Hagmann et al., 2008; Lu et al., 2012; Wu et al., 2017). In the present study, we not only reinforced this finding from the aspect of fast DMN dynamics but also provided a possible dynamic substrate for this separation of the DMN structure. As a key component of the DMN, the orbital frontal cortex has historically been posited to integrate interoceptive and exteroceptive information from multisensory stimuli to process information about the internal and external bodily milieu(Ongur & Price, 2000). Accordingly, we speculated that the high-activity micropattern aDMN might make inferences and guide actions in a timely and environmentally relevant manner.

Furthermore, the retrosplenial cortex (RSC) located in the posterior DMN, another

key area in the DMN, has extensive connections and is topographically organized with the hippocampal formation. The projections between the RSC and hippocampal formation provide an important pathway that regulates learning, memory and emotional behavior(Wyss & Vangroen, 1992). Furthermore, the hippocampal formation is a limbic structure that forms direct or indirect connections to other DMN regions. Therefore, the high-activity micropattern pDMN detected in the present study might be associated with memory and emotional behavior. Additionally, both the aDMN and pDMN were strongly phase locked to the up state of anterior DMN activity and the down state of posterior DMN activity during the SWS stage, indicating that they may reflect similar performances for the up-down states of slow oscillations during DMN dynamics. Moreover, these two high-activity micropatterns together accounted for more than 70% of the time in the resting state, which helps explain why the brain requires high basal cerebral blood flow and metabolism for spontaneous activity(Marcus E Raichle & Mintun, 2006). It should be noted that the structure of DMN could also be split into dorsal and ventral branches according to the dorsal and medial temporal regions of RSC and hippocampus in human brain(Chen, Glover, Greicius, & Chang, 2017; Shirer, Ryali, Rykhlevskaia, Menon, & Greicius, 2012). However, the rat DMN is commonly divided into the anterior and posterior subsystems for the anatomical difference with human DMN(Marcus E. Raichle, 2015).

In addition, we observed a low-activity micropattern (i.e., cDMN) in DMN dynamics that was widely distributed in all conscious stages during wakefulness and

sleep. In the cDMN, all DMN regions displayed relatively lower levels of activity, implicating that the cDMN could be the silent state for DMN activity in which all the DMN regions prefer relaxations and are prepared for the next excitation. However, the cDMN was the only micropattern in which all DMN regions operated in the same manner in regards to DMN dynamics. Thus, the appearance of the cDMN suggested that a working mode for DMN with low energy exists, but this concept requires further study.

The balance of dynamic DMN configurations supports consciousness during wakefulness. Based on accumulating evidence, DMN activity is tightly correlated with consciousness levels in health and disease(Buckner, Andrews-Hanna, & Schacter, 2008; Kapogiannis et al., 2014; Panda et al., 2016; Vanhaudenhuyse et al., 2010). In the AWAKE stage, all the CAMPs showed similar features, and the dynamic transitions among them were not significantly different. These similarities illustrated a balanced dynamic configuration among these CAMPs during fast gamma activity in the DMN at rest. The DMN is a key network involved in integrating high-order information from multiple sensory modalities based on numerous projections from variable somatic cortex and core limbic structures (HIP and amygdala) to the DMN regions(Heidbreder & Groenewegen, 2003; Reep, Chandler, King, & Corwin, 1994). These projections might provide the anatomical substrate for the correlation of DMN activity with consciousness levels, which are largely believed to be determined by global levels of arousal regulated by the brainstem via the reticular activating system (RAS)(Delano-Wood et al., 2015). Accordingly, the identified balance of DMN

dynamics might be a competitive product between the integration and differentiation of DMN activity in maintaining consciousness during wakefulness(Cavanna, Vilas, Palmucci, & Tagliazucchi, 2018; Tononi, 2004; Tononi, Boly, Massimini, & Koch, 2016). Furthermore, this balance of dynamic configurations also indicated that the DMN might function in multistable regimes and revealed the potential neural mechanism by which DMN activity supports cognitive functions in the resting state(Andrews-Hanna, 2012; Buckner et al., 2008).

Functional reorganization of dynamic DMN configurations during sleep. Compared to the resting stage, the SWS stage was always shown to be accompanied by reduced brain activity, while commensurate brain activity has been reported in the REM sleep stage(Hobson, 2009; Horovitz et al., 2008). Consistent alterations in the average brain activity associated with CAMPs during DMN dynamics were also observed in our study, suggesting that the activities of CAMPs might also reveal the changes in consciousness during wakefulness and sleep. However, the reduced activities of all CAMPs might not sufficiently explain the decrease in DMN activity observed during deep sleep due to the stable spatial structures of these CAMPs during wakefulness and sleep. This decrease in activity might result from the increased occurrence probability of the cDMN and the decreased probabilities of the other two high-activity micropatterns. These inversely changed occurrence probabilities in different CAMPs revealed the neural mechanism of reduced activity, as the DMN regions were shown to prefer the low-activity state during deep sleep(Bazhenov, Timofeev, Steriade, & Sejnowski, 2002; Diekelmann & Born, 2010).

The balance of dynamic DMN configurations was also disrupted during sleep, indicating the functional reorganization of DMN dynamics., and functional reorganization was shown to subsequently lead to a loss of consciousness in different sleep stages(Tononi, 2004; Tononi et al., 2016). In the REM sleep stage, the dynamic transitions between the aDMN and pDMN increased, indicating more communication between anterior and posterior DMN regions. These communications between anterior and posterior DMN regions might be crucial for primary consciousness, which is thought to be preserved in the REM sleep stage(Hobson, 2009). Moreover, these communications in the DMN displayed both top-down and bottom-up mechanisms, both of which are important for information processing in the brain(Buschman & Miller, 2007; Theeuwes, 2010), and enhancement of these mechanisms might help elucidate the neurophysiological basis underlying the preservation of primary consciousness during REM sleep.

In the SWS stage, the changes in the dynamic transitions among CAMPs differed, as the dynamic transitions between the low-activity micropattern and two high-activity micropatterns increased significantly. Additionally, a strong phasic relationship was observed between CAMPs and the up-down states during slow oscillations of the anterior and posterior DMNs, and these two types of CAMPs corresponded to different up-down states. Accordingly, the dynamic transitions between the low-activity micropattern and two high-activity micropatterns were deemed to be within up-down states in the DMN. The dominant transitions of up-down states in deep sleep further suggested the physiological importance of these

increased dynamic transitions. However, the dynamic transitions within the two high-activity micropatterns decreased in the SWS stage. These reductions supported our hypothesis that communications between anterior and posterior DMN regions are important for primary consciousness since both higher cognitive functions and primary consciousness are lost during deep sleep(Hobson & Pace-Schott, 2002). The loss of higher cognitive functions might not be caused by the change in a single type of dynamic transition within pairs of CAMPs. We speculated that the balance of dynamic DMN configurations was the underlying neural mechanism supporting higher cognitive functions, which emerged during wakefulness and were deactivated during sleep. The coordination and cooperation of all CAMPs played a core role in the ability of the DMN to perform higher cognitive functions.

Based on these findings, we propose a three-state model to describe the relationship between DMN micropatterns and the underlying consciousness levels observed during wakefulness and sleep. As shown in Fig. 6, the three CAMPs involved in DMN dynamics are the basis of this model, and their interactions refer to the underlying mechanism regulating the consciousness level observed in distinct stages. Equal communications among the three CAMPs support conscious awareness in the AWAKE stage. The communications between the low-activity micropattern (i.e., cDMN) and each high-activity micropattern (i.e., aDMN and pDMN) are important for the SWS stage characterized by a low level of consciousness. However, during REM sleep with primary consciousness, communications within high-activity micropatterns are predominant.

According to the proposed three-state model, we speculate that preservation of conscious awareness requires not only information processing between anterior and posterior DMN regions but also that all DMN regions remain silent and relaxed during this process. Information processing within anterior and posterior DMN regions is mediated by up-down and bottom-up mechanisms and is vital for supporting conscious awareness and primary consciousness. Absence of this process could lead to the loss of consciousness in the SWS stage, and this process alone would result in the consciousness level of the REM sleep stage that exists as primary consciousness. This phenomenon highlights the importance of the silent pattern for all DMN regions during the resting state with conscious awareness.

In addition, the consciousness in humans not only depends on the anterior-posterior integration with DMN regions, but also with the fronto-parietal task-positive executive and attention networks. Moreover, the connections between DMN and task positive networks also play critical roles in supporting consciousness. Because of the limitation of neuroimaging measure, the current work just descripts the associations between DMN dynamics and consciousness with a three-state model. The roles of integrations between DMN and other networks could not be explored currently. Further work could validate our model with DMN activity during wakefulness-sleep cycle and furtherly track the roles of integrations among different ICNs in consciousness with human EEG signals.

Methodological Perspectives. Consistent with the promising microstate analysis of EEG/LFP signals(Michel & Koenig, 2018), the CAMP analysis reported herein also

assumes that brain activity consists of several distinct instantaneous patterns. The difference is that the CAMP method focuses on the nature of brain activity in different regions and extracts micropatterns from envelope signals. Envelope signals imply temporal alterations in brain power, and their decomposition directly reveals brain rhythm dynamics. In addition, the coactive patterns analyzed in the CAMP method were chosen based on the distributions of extreme values in the envelope signals of brain regions, which differs from the method used in microstate analysis. Local extreme values in envelope signals represent the instantaneous higher/lower activities of brain regions followed by contrasting changes in activity. Therefore, the derived coactive patterns were considered to be the activity patterns leading to inversion of activity among regions in specific brain networks. Therefore, we postulate that this proposed CAMP method will help researchers elucidate coactive micropatterns in specific brain networks and reveal additional underlying information about fast brain dynamics.

Limitation. Although we reveal several interesting findings in the current work, some limitations exist that should be taken into consideration. First, the rat DMN is slightly anatomically different from the human DMN, and our findings in rat DMN dynamics need to be validated in the human DMN during wakefulness and sleep. In addition, the present work revealed the dynamic configurations of DMN activity in only the gamma band, and different frequency bands have corresponding physiological roles. The relationships between the DMN dynamics in other frequency bands and consciousness should be investigated in futures studies.

Conclusion

The DMN is believed to be associated with neural mechanisms of consciousness, while the fast dynamics of DMN activity in different conscious stages are still unclear. We highlighted that the fast dynamics of DMN activity during wakefulness and sleep shared structurally stable CAMPs, while their dynamic configurations were specific to different levels of consciousness. Our findings indicated the reorganization of DMN dynamics during wakefulness and sleep and proposed a three-state model to reveal the fundamental neural associations between DMN activity and consciousness.

Acknowledgments

We thank Professor Pedro A. Valdes-Sosa for the valuable discussions and suggestions regarding this work.

Authorship Confirmation Statement

Y.X., D.Y., C.Z., and D.G. designed the research; Y.C., M.L., and W.J. performed the research; Y.C., M.L., B.B., and H.L. analyzed the data; and C.Y., B.B., D.G., and D.Y. wrote the paper.

Authors' Disclosure Statement

The authors declare that no competing financial interests exist.

Funding Statement

This study was supported by the National Natural Science Foundation of China (grant nos. 81861128001, 61527815, 31771149, 61761166001, 61871420, 11975194 and 81901366), the Sichuan Science and Technology Program (grant no. 2018HH0003), and the 111 project (grant no. B12027).

References

Andrews-Hanna, J. R. (2012). The Brain's Default Network and its Adaptive Role in Internal Mentation. *Neuroscientist*, *18*(3), 251–270. https://doi.org/10.1016/j.neuroimage.2013.08.045.The

Bazhenov, M., Timofeev, I., Steriade, M., & Sejnowski, T. J. (2002). Model of thalamocortical slow-wave sleep oscillations and transitions to activated states. *The Journal of Neuroscience*, *22*(19), 1.

Beckmann, C. F., DeLuca, M., Devlin, J. T., & Smith, S. M. (2005). Investigations into resting-state connectivity using independent component analysis. *Philosophical Transactions of the Royal Society B: Biological Sciences*, *360*(1457), 1001–1013. https://doi.org/10.1098/rstb.2005.1634

Brett L. Foster, Mohammad Dastjerdi, and J. P. (2012). Neural populations in human posteromedial cortex display opposing responses during memory and numerical processing. *Proceedings of the National Academy of Sciences*, *109*, 15514–15519. https://doi.org/10.1073/pnas.1206580109/-/DCSupplemental.www.pnas.org/cgi/doi/10.1073/pnas.1206580109

Buckner, R. L., Andrews-Hanna, J. R., & Schacter, D. L. (2008). The brain's default network: Anatomy, function, and relevance to disease. *Annals of the New York Academy of Sciences*, *1124*, 1–38. https://doi.org/10.1196/annals.1440.011

Buschman, T. J., & Miller, E. K. (2007). Top-Down Versus Bottom-Up Control of Attention in the Prefrontal and. *Science*, *315*(March), 1860–1863.

https://doi.org/10.1126/science.1138071

Cavanna, F., Vilas, M. G., Palmucci, M., & Tagliazucchi, E. (2018). Dynamic functional connectivity and brain metastability during altered states of consciousness. *NeuroImage*, *180*, 383–395. https://doi.org/10.1016/j.neuroimage.2017.09.065

Chen, J. E., Glover, G. H., Greicius, M. D., & Chang, C. (2017). Dissociated patterns of anti-correlations with dorsal and ventral default-mode networks at rest. *Human Brain Mapping*, *38*(5), 2454–2465. https://doi.org/10.1002/hbm.23532

Crunelli, V., & Hughes, S. W. (2010). The slow (1 Hz) rhythm of non-REM sleep: A dialogue between three cardinal oscillators. *Nature Neuroscience*, *13*(1), 9–17. https://doi.org/10.1038/nn.2445

Cui, Y., Yu, S., Zhang, T., Zhang, Y., Xia, Y., Yao, D., & Guo, D. (2018). Altered activity and information flow in the default mode network of pilocarpine-induced epilepsy rats. *Brain Research*, *1696*, 71–80. https://doi.org/10.1016/j.brainres.2018.05.012

Delano-Wood, L., Bangen, K. J., Sorg, S. F., Clark, A. L., Schiehser, D. M., Luc, N., … Bigler, E. D. (2015). Brainstem white matter integrity is related to loss of consciousness and postconcussive symptomatology in veterans with chronic mild to moderate traumatic brain injury. *Brain Imaging and Behavior*, *9*(3), 500–512. https://doi.org/10.1007/s11682-015-9432-2

Diekelmann, S., & Born, J. (2010). The memory function of sleep. *Nature Reviews. Neuroscience*, *11*(2), 114–126. https://doi.org/10.1038/nrn2762

Foster, B. L., Rangarajan, V., Shirer, W. R., & Parvizi, J. (2015). Intrinsic and task-dependent coupling of neuronal population activity in human parietal cortex. *Neuron*, *86*(2), 578–590. https://doi.org/10.1016/j.neuron.2015.03.018

Fox, K. C. R., Foster, B. L., Kucyi, A., Daitch, A. L., & Parvizi, J. (2018). Intracranial Electrophysiology of the Human Default Network. *Trends in Cognitive Sciences*. https://doi.org/10.1016/j.tics.2018.02.002

Fox, M. D., Snyder, A. Z., Vincent, J. L., Corbetta, M., Essen, C. Van, Raichle, M. E., … Raichle, M. E. (2016). Networks Linked references are available on JSTOR for this article□: The human brain is intrinsically organized into dynamic , anticorrelated functional networks. *Proceedings of the National Academy of Sciences of the United States of America*, (May).

Gretenkord, S., Olthof, B. M. J., Stylianou, M., Rees, A., Gartside, S. E., & LeBeau, F. E. N. (2020). Electrical stimulation of the ventral tegmental area evokes sleep-like state transitions under urethane anaesthesia in the rat medial prefrontal cortex via dopamine D1-like receptors. *European Journal of Neuroscience*, *52*(2), 2915–2930. https://doi.org/10.1111/ejn.14665

Gusnard, D. A., Akbudak, E., Shulman, G. L., & Raichle, M. E. (2001). Medial prefrontal cortex and self-referential mental activity: Relation to a default mode of brain function. *Proceedings of the National Academy of Sciences of the United States of America*, *98*(7), 4259–4264. https://doi.org/10.1073/pnas.071043098

Hagmann, P., Cammoun, L., Gigandet, X., Meuli, R., Honey, C. J., Van Wedeen, J., & Sporns, O. (2008). Mapping the structural core of human cerebral cortex.

PLoS Biology, *6*(7), 1479–1493. https://doi.org/10.1371/journal.pbio.0060159

Heidbreder, C. A., & Groenewegen, H. J. (2003). The medial prefrontal cortex in the rat: Evidence for a dorso-ventral distinction based upon functional and anatomical characteristics. *Neuroscience and Biobehavioral Reviews*, *27*(6), 555–579. https://doi.org/10.1016/j.neubiorev.2003.09.003

Hobson, J. A. (2009). REM sleep and dreaming: Towards a theory of protoconsciousness. *Nature Reviews Neuroscience*, *10*(11), 803–814. https://doi.org/10.1038/nrn2716

Hobson, J. A., & Pace-Schott, E. F. (2002). The cognitive neuroscience of sleep: Neuronal systems, consciousness and learning. *Nature Reviews Neuroscience*, *3*(9), 679–693. https://doi.org/10.1038/nrn915

Holcman, D., & Tsodyks, M. (2006). The emergence of up and down states in cortical networks. *PLoS Computational Biology*, *2*(3), 174–181. https://doi.org/10.1371/journal.pcbi.0020023

Horovitz, S. G., Fukunaga, M., De Zwart, J. A., Van Gelderen, P., Fulton, S. C., Balkin, T. J., & Duyn, J. H. (2008). Low frequency BOLD fluctuations during resting wakefulness and light sleep: A simultaneous EEG-fMRI study. *Human Brain Mapping*, *29*(6), 671–682. https://doi.org/10.1002/hbm.20428

Hsu, L.-M., Liang, X., Gu, H., Brynildsen, J. K., Stark, J. A., Ash, J. A., … Yang, Y. (2016). Constituents and functional implications of the rat default mode network. *Proceedings of the National Academy of Sciences*, *113*(31), E4541–E4547. https://doi.org/10.1073/pnas.1601485113

Huang, S. M., Wu, Y. L., Peng, S. L., Peng, H. H., Huang, T. Y., Ho, K. C., & Wang, F. N. (2016). Inter-Strain Differences in Default Mode Network: A Resting State fMRI Study on Spontaneously Hypertensive Rat and Wistar Kyoto Rat. *Scientific Reports*, *6*(February), 1–9. https://doi.org/10.1038/srep21697

Jercog, D., Roxin, A., Barthó, P., Luczak, A., Compte, A., & De La Rocha, J. (2017). UP-DOWN cortical dynamics reflect state transitions in a bistable network. *ELife*, *6*, 1–33. https://doi.org/10.7554/eLife.22425

Ji, D., & Wilson, M. A. (2007). Coordinated memory replay in the visual cortex and hippocampus during sleep. *Nature Neuroscience*, *10*(1), 100–107. https://doi.org/10.1038/nn1825

Jing, W., Guo, D., Zhang, Y., Guo, F., Valdés-Sosa, P. A., Xia, Y., & Yao, D. (2017). Reentrant information flow in electrophysiological rat default mode network. *Frontiers in Neuroscience*, *11*(FEB), 1–12. https://doi.org/10.3389/fnins.2017.00093

Kapogiannis, D., Reiter, D. A., Willette, A. A., & Mattson, M. P. (2014). Dynamic functional connectivity of the default mode network tracks daydreaming. *NeuroImage*, *100*, 112–119. https://doi.org/10.1016/j.neuroimage.2012.09.029.Posteromedial

Karim Jerbi*†, R., V. J., Tomas，, O., Dalal, S. S., Julien Jung, D. H., Minotti, L., … Lachaux, and J.-P. (2010). Exploring the electrophysiological correlates of the default-mode network with intracerebral EEG. *Frontiers in Systems Neuroscience*, *4*(June), 1–9. https://doi.org/10.3389/fnsys.2010.00027

Larson-Prior, L. J., Zempel, J. M., Nolan, T. S., Prior, F. W., Snyder, A., & Raichle, M. E. (2009). Cortical network functional connectivity in the descent to sleep. *Proceedings of the National Academy of Sciences of the United States of America*, *106*(11), 4489–4494. https://doi.org/10.1073/pnas.0900924106

Liu, Q., Farahibozorg, S., Porcaro, C., Wenderoth, N., & Mantini, D. (2017). Detecting large-scale networks in the human brain using high-density electroencephalography. *Human Brain Mapping*, *38*(9), 4631–4643. https://doi.org/10.1002/hbm.23688

Liu, X., & Duyn, J. H. (2013). Time-varying functional network information extracted from brief instances of spontaneous brain activity. *Proceedings of the National Academy of Sciences of the United States of America*, *110*(11), 4392–4397. https://doi.org/10.1073/pnas.1216856110

Logothetis, N. K., Pauls, J., Augath, M., Trinath, T., & Oeltermann, A. (2001). Neurophysiological investigation of the basis of the fMRI signal. *Nature*, *412*(6843), 150–157. https://doi.org/10.1038/35084005

Logothetis, Nikos K. (2002). The neural basis of the blood-oxygen-level-dependent functional magnetic resonance imaging signal. *Philosophical Transactions of the Royal Society B: Biological Sciences*, *357*(1424), 1003–1037. https://doi.org/10.1098/rstb.2002.1114

Lőrincz, M. L., Gunner, D., Bao, Y., Connelly, W. M., Isaac, J. T. R., Hughes, S. W., & Crunelli, V. (2015). A distinct class of slow (~0.2–2 Hz) intrinsically bursting layer 5 pyramidal neurons determines UP/DOWN state dynamics in the

neocortex. *Journal of Neuroscience*, *35*(14), 5442–5458. https://doi.org/10.1523/JNEUROSCI.3603-14.2015

Lu, H., Zou, Q., Gu, H., Raichle, M. E., Stein, E. A., & Yang, Y. (2012). Rat brains also have a default mode network. *Proceedings of the National Academy of Sciences of the United States of America*, *109*(10), 3979–3984. https://doi.org/10.1073/pnas.1200506109

Magri, C., Schridde, U., Murayama, Y., Panzeri, S., & Logothetis, N. K. (2012). The Amplitude and Timing of the BOLD Signal Reflects the Relationship between Local Field Potential Power at Different Frequencies. *The Journal of Neuroscience*, *32*(4), 1395–1407. https://doi.org/10.1523/JNEUROSCI.3985-11.2012

Michel, C. M., & Koenig, T. (2018). EEG microstates as a tool for studying the temporal dynamics of whole-brain neuronal networks: A review. *NeuroImage*, *180*(November 2017), 577–593. https://doi.org/10.1016/j.neuroimage.2017.11.062

Ongur, D., & Price, J. (2000). The Organization of Networks within the Orbital and Medial Prefrontal Cortex of Rats, Monkeys and Humans. *Cerebral Cortex*, *10*(3), 206–219. https://doi.org/10.1093/cercor/10.3.206

Ossandon, T., Jerbi, K., Vidal, J. R., Bayle, D. J., Henaff, M.-A., Jung, J., … Lachaux, J.-P. (2011). Transient Suppression of Broadband Gamma Power in the Default-Mode Network Is Correlated with Task Complexity and Subject Performance. *Journal of Neuroscience*, *31*(41), 14521–14530.

https://doi.org/10.1523/JNEUROSCI.2483-11.2011

Panda, R., Bharath, R. D., Upadhyay, N., Mangalore, S., Chennu, S., & Rao, S. L. (2016). Temporal Dynamics of the Default Mode Network Characterize Meditation-Induced Alterations in Consciousness. *Frontiers in Human Neuroscience*, *10*(July), 1–12. https://doi.org/10.3389/fnhum.2016.00372

Perez-Zabalza, M., Reig, R., Manrique, J., Jercog, D., Winograd, M., Parga, N., & Sanchez-Vives, M. V. (2020). Modulation of cortical slow oscillatory rhythm by GABAB receptors: an in vitro experimental and computational study. *Journal of Physiology*, *598*(16), 3439–3457. https://doi.org/10.1113/JP279476

Raichle, M E, MacLeod, A. M., Snyder, A. Z., Powers, W. J., Gusnard, D. A., & Shulman, G. L. (2001). A default mode of brain function. *Proceedings of the National Academy of Sciences of the United States of America*, *98*(2), 676–682. https://doi.org/10.1073/pnas.98.2.676

Raichle, Marcus E. (2015). The Brain's Default Mode Network. *Annual Review of Neuroscience*, *38*(1), 433–447. https://doi.org/10.1146/annurev-neuro-071013-014030

Raichle, Marcus E. (2015). The Brain ' s Default Mode Network. *Annual Review Neuroscience*, (April), 413–427. https://doi.org/10.1146/annurev-neuro-071013-014030

Raichle, Marcus E, & Mintun, M. A. (2006). Brain work and brain imaging. *Annual Review of Neuroscience*, *29*, 449–476. https://doi.org/10.1146/annurev.neuro.29.051605.112819

Reep, R. L., Chandler, H. C., King, V., & Corwin, J. V. (1994). Rat posterior parietal cortex: topography of corticocortical and thalamic connections. *Experimental Brain Research*, *100*(1), 67–84. https://doi.org/10.1007/BF00227280

Rosazza, C., & Minati, L. (2011). Resting-state brain networks: Literature review and clinical applications. *Neurological Sciences*, *32*(5), 773–785. https://doi.org/10.1007/s10072-011-0636-y

Sämann, P. G., Wehrle, R., Hoehn, D., Spoormaker, V. I., Peters, H., Tully, C., … Czisch, M. (2011). Development of the brain's default mode network from wakefulness to slow wave sleep. *Cerebral Cortex*, *21*(9), 2082–2093. https://doi.org/10.1093/cercor/bhq295

Scheering, R., Koopmans, P. J., Van Mourik, T., Jensen, O., & Norris, D. G. (2016). The relationship between oscillatory EEG activity and the laminar-specific BOLD signal. *Proceedings of the National Academy of Sciences of the United States of America*, *113*(24), 6761–6766. https://doi.org/10.1073/pnas.1522577113

Shirer, W. R., Ryali, S., Rykhlevskaia, E., Menon, V., & Greicius, M. D. (2012). Decoding subject-driven cognitive states with whole-brain connectivity patterns. *Cerebral Cortex*, *22*(1), 158–165. https://doi.org/10.1093/cercor/bhr099

Theeuwes, J. (2010). Top-down and bottom-up control of visual selection. *Acta Psychologica*, *135*(2), 77–99. https://doi.org/10.1016/j.actpsy.2010.02.006

Tononi, G. (2004). *An information integration theory of consciousness. BMC neuroscience* (Vol. 5). BioMed Central. https://doi.org/10.1186/1471-2202-5-42

Tononi, G., Boly, M., Massimini, M., & Koch, C. (2016, July 26). Integrated information theory: From consciousness to its physical substrate. *Nature Reviews Neuroscience*. https://doi.org/10.1038/nrn.2016.44

Tu, W., Ma, Z., Ma, Y., Dopfel, D., & Zhang, N. (2020). Suppressing Anterior Cingulate Cortex Modulates Default Mode Network and Behavior in Awake Rats. *Cerebral Cortex*, 1–12. https://doi.org/10.1093/cercor/bhaa227

Upadhyay, J., Baker, S. J., Chandran, P., Miller, L., Lee, Y., Marek, G. J., … Day, M. (2011). Default-Mode-Like Network Activation in Awake Rodents. *PLoS ONE*, *6*(11). https://doi.org/10.1371/journal.pone.0027839

Vanhaudenhuyse, A., Noirhomme, Q., Tshibanda, L. J. F., Bruno, M. A., Boveroux, P., Schnakers, C., … Boly, M. (2010). Default network connectivity reflects the level of consciousness in non-communicative brain-damaged patients. *Brain*, *133*(1), 161–171. https://doi.org/10.1093/brain/awp313

Vidaurre, D., Smith, S. M., & Woolrich, M. W. (2017). Brain network dynamics are hierarchically organized in time. *Proceedings of the National Academy of Sciences*, 201705120. https://doi.org/10.1073/pnas.1705120114

Wu, X. jie, Zeng, L. L., Shen, H., Yuan, L., Qin, J., Zhang, P., & Hu, D. (2017). Functional network connectivity alterations in schizophrenia and depression. *Psychiatry Research - Neuroimaging*, *263*(March), 113–120. https://doi.org/10.1016/j.pscychresns.2017.03.012

Wyss, J. M., & Vangroen, T. (1992). Connections between the retrosplenial cortex and the hippocampal-formation in the rat - a review. *Hippocampus*, *2*(1), 1–12.

https://doi.org/10.1002/hipo.450020102

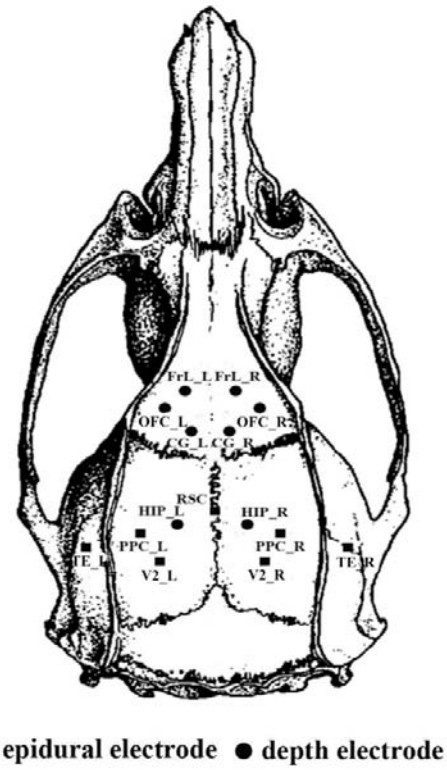

Figure 1. The placement of 15 intracranial electrodes.

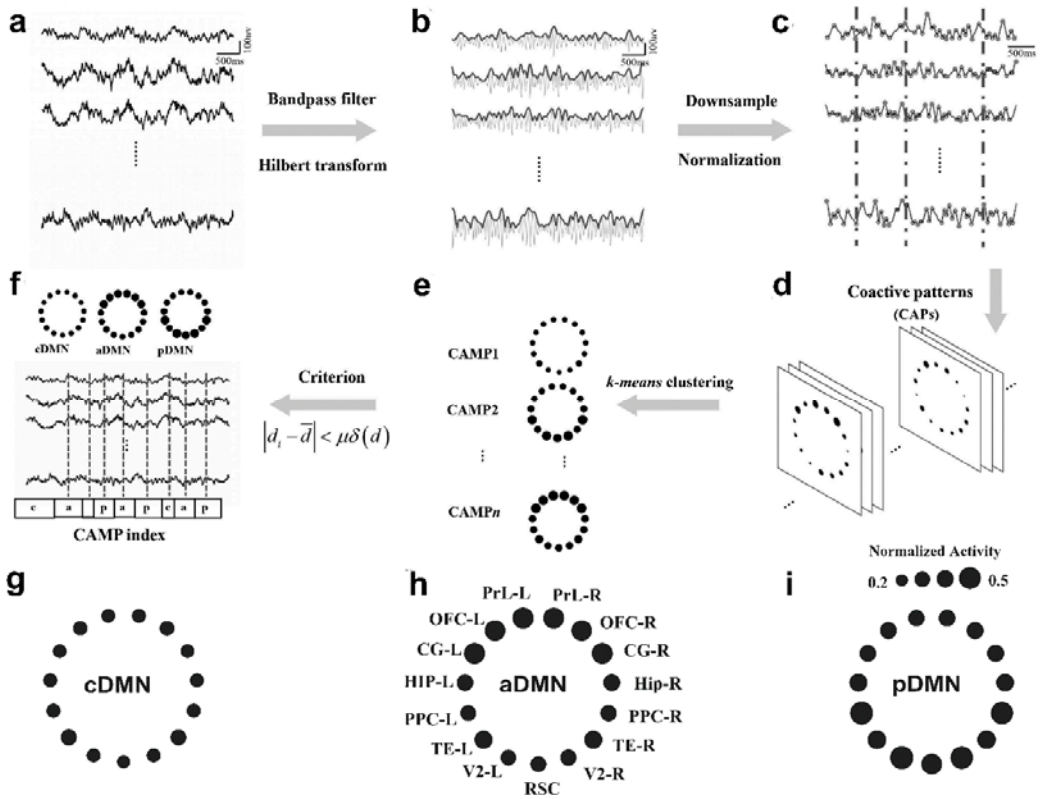

Figure 2. Schematic of the CAMP procedure and three CAMPs of gamma activity in the DMN during wakefulness and sleep. (a) The original LFPs. (b) The envelope signals (blue lines) were extracted by applying the Hilbert transform to the bandpass-filtered signals (gray lines). (c) All the envelope signals were downsampled (blue lines), and the extreme values were detected as the active points for each channel (red dots). The dotted lines suggest the coactive points in which more than N (N=7 in the present study) active points were observed across DMN regions. (d) The coactive patterns were the maps of activity of all DMN regions at coactive points. (e) The k-means clustering algorithm was applied to all coactive patterns to detect the CAMPs. (f) A criterion was employed to remove several coactive points and increase the aggregation of the CAMPs. The final CAMPs and CAMP index detected in this step were subjected to further analyses. (g) Spatial structure of the common low-activity level micropattern (cDMN). (h) Spatial structure of the anterior high-activity level micropattern (aDMN). (i) Spatial structure of the posterior high-activity level micropattern (pDMN).

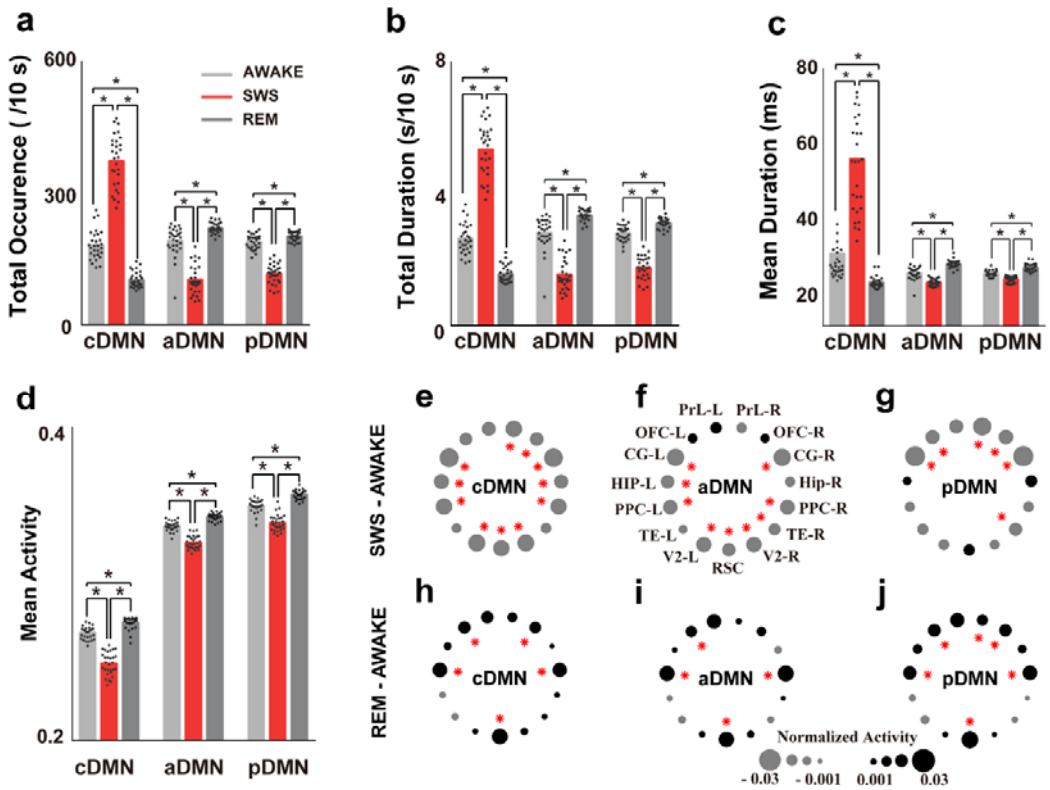

Figure 3. Comparisons of the temporal features and activity levels of each CAMP during wakefulness and sleep. (a) Comparisons of the total occurrence of each CAMP in different conscious stages. The dots represent the values obtained from 29 rats, and the black stars indicate significant differences with a corrected p<0.001. (b) Comparisons of the total duration. (c) Comparisons of the mean duration. (d) Comparisons of the mean DMN activity during wakefulness and sleep for different CAMPs. (e-j) Comparisons of activity in DMN nodes for different CAMPs across different conscious stages: (e and h) cDMN, (f and i) aDMN, and (g and j) pDMN. Gray dots indicate decreased normalized activity and black dots indicate increased normalized activity. The size of the dot reflects the value of the difference, and the red stars indicate significance differences with a corrected p<0.001.

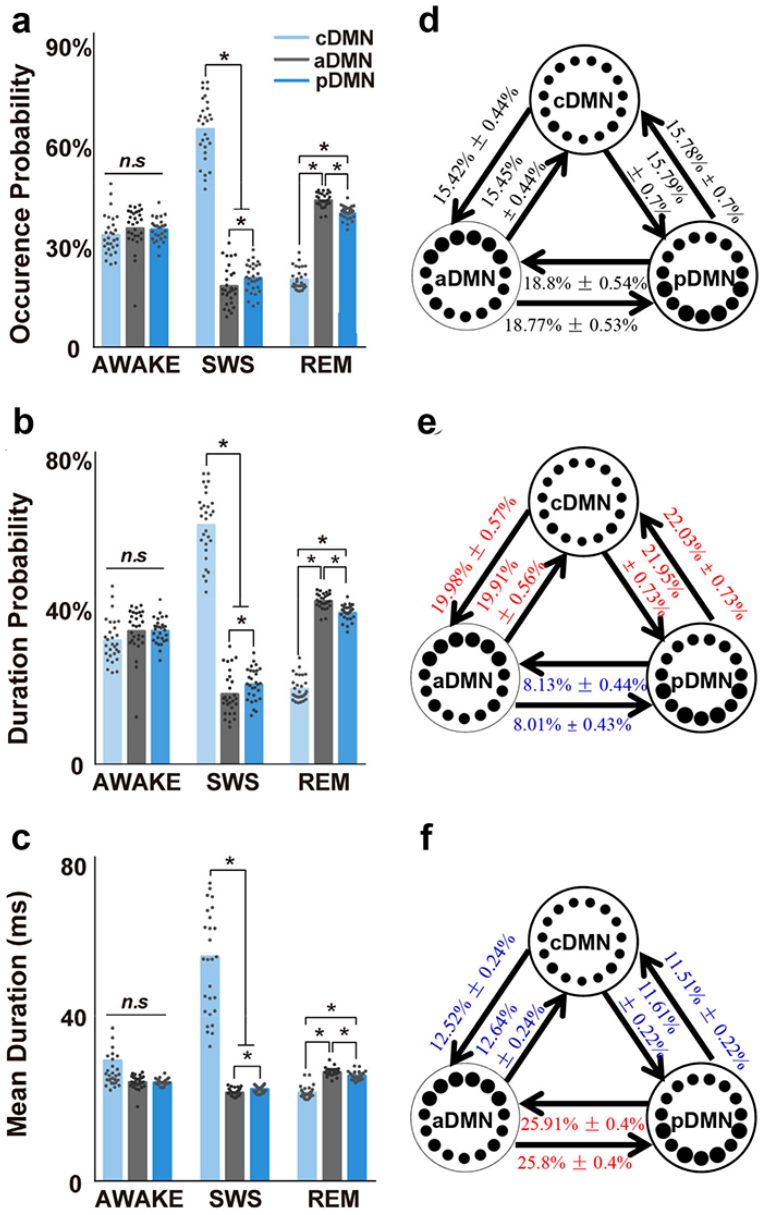

Figure 4. Characteristics of CAMPs and the transitions among them in different stages of consciousness during wakefulness and sleep. (a) Comparisons of the occurrence probability for all CAMPs in the three stages. The black dots indicate the values of the occurrence probability obtained from 29 rats in different CAMPs and stages. The black stars indicate significant differences with a corrected $p<0.001$. (b) Comparisons of the duration probability. (c) Comparisons of the mean duration. (d-f) The transition structures among CAMPs for the AWAKE (d), SWS (e) and REM sleep stages (f). All the numbers indicate the mean TPs calculated for the 29 rats and the standard deviation. The numbers in blue indicate a significantly lower transition probability than observed in the AWAKE stage, and the numbers in red indicate a significantly higher transition probability. The significance level is a corrected $p<0.001$.

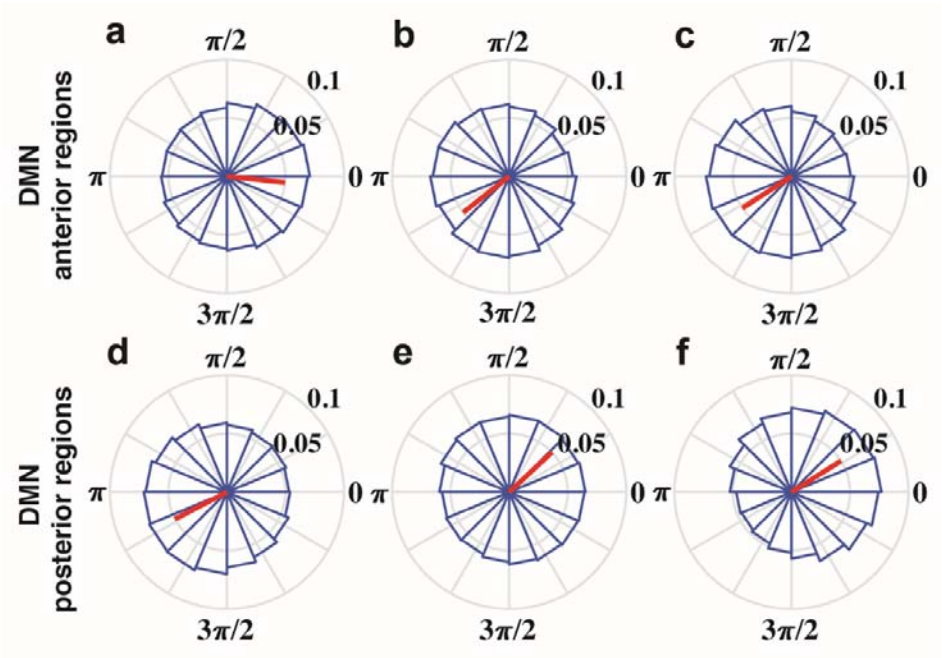

Figure 5. Phase locking relationship between each CAMP with slow oscillations in the SWS stage. (a-c) The phase locking relationships between the cDMN (a), aDMN (b) and pDMN (c) with the slow oscillations in anterior DMN regions. (d-f) The phase locking relationships between the cDMN (d), aDMN (e) and pDMN (f) with the slow oscillations in posterior DMN regions. The red lines showed the significant directionality with Rayleigh test $p<0.001$.

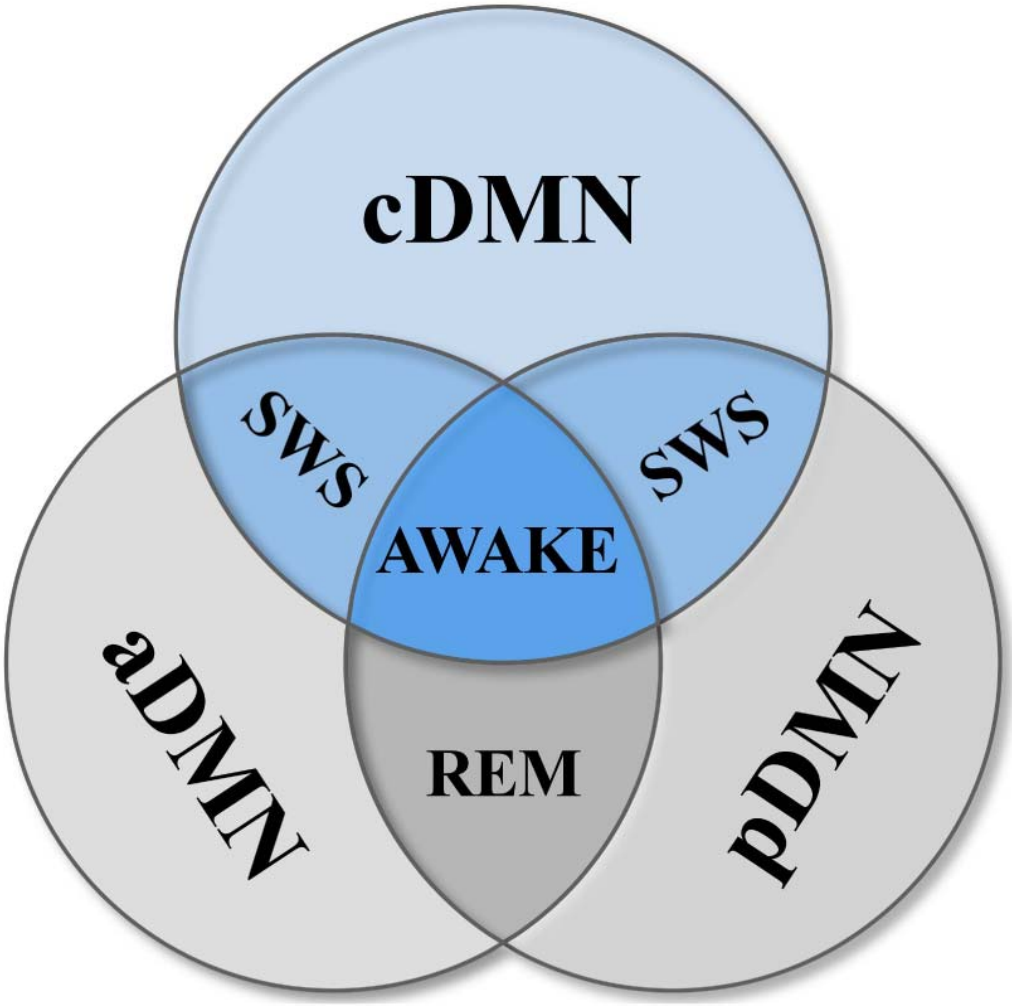

Figure 6. The three-state model of the consciousness levels during wakefulness and sleep. The AWAKE stage requires the cooperation of all three CAMPs, while the SWS stage requires communications between the low-activity micropattern (cDMN) and the high-activity micropatterns (aDMN or pDMN). The REM sleep stage requires interactions within the two high-activity micropatterns.